SUM4Re

Creating materials banks
from digital urban mining

D2.2 AHS methodological framework acquisition

PUBLIC

VERSION 1.0

28 October 2025

Associated with document Ref. 101129961

Funded by the European Union. Views and opinions expressed are however those of the author(s) only and do not necessarily reflect those of the European Union. Neither the European Union nor the granting authority can be held responsible for them.

Funded by the European Union

SUM4Re

Creating materials banks from digital urban mining

Deliverable ID	D2.2
Deliverable name	AHS methodological framework acquisition
Lead partner	VTT
Contributors	THUAS, SINTEF, STORE NORKSE

PUBLIC

Funded by the European Union

DOCUMENT INFORMATION

Document name	D2.2 AHS methodological framework acquisition
Version	1.0
Due date	31/10/2025
Report date	27/10/2025
Number of pages	27
Lead Author	Francisco Senna Vieira (VTT)
Other Authors	-
Dissemination level	Public

REVISION HISTORY

Rev.	Date	Description of revision
0.1	02/10/2025	Initial version
0.2	15/10/2025	Version after technical revision
1.0	27/10/2025	Final version (approved)

DOCUMENT APPROVAL

Written	Francisco Senna Vieira (VTT)	02/10/2025
Revised	Pablo J. Arauzo (OLAR), Rizal Sebastian (THUAS)	From 02/10/2025 to12/10/2025
Approved	Pedro Arias Sánchez (UVIGO, Project Coordinator)	27/10/2025

EXECUTIVE SUMMARY

This deliverable describes the data collection procedures using the VTT active hyperspectral sensor (AHS) and the laboratory reference hyperspectral camera (Specim). We collected data from reference wood samples relevant to the pilot tests, as well as samples obtained from the field (in the case of the Nordic pilot). We submitted some of the samples to high humidity conditions and tested the effect of humidity in the signals of both AHS and the conventional hyperspectral camera.

We present here exploratory data analysis results related to the hyperspectral images collected with both instruments. The data analysis includes dimensionality reduction and clustering methods such as principal component analysis (PCA), uniform manifold approximation and projection (UMAP) to identify patterns existing in the data regardless of reference information. It also includes preliminary investigations to the question of detecting mould in the wood, which is done applying the multivariate curve resolution alternating least squares (MCR-ALS) method to the hyperspectral data collected from the samples of high humidity. We also evaluate qualitatively the sensitivity of AHS to detect moisture in wood samples.

GLOSSARY

Terms, Abbreviations, and Acronyms

AHS	Active hyperspectral sensor
AI	Artificial intelligence
ANN	Artificial neural networks
CH	Carbon-hydrogen bond
GA	Grant Agreement
HSI	Hyperspectral imaging
MCR-ALS	Multivariate curve resolution alternating least squares
MEMS-FPI	Microlectromechanical Fabry-Perot interferometer
NIR	Near infrared
OH	Oxygen-hydrogen bond
PCA	Principal component analysis
PLS	Partial least squares
PLS-DA	Partial least squares discriminant analysis
SNR	Signal-to-noise ratio
SVM	Support vector machine
SWIR	Short-wave infrared
UC	Use case

TABLE OF CONTENTS

DOCUMENT INFORMATION **3**
REVISION HISTORY **3**
DOCUMENT APPROVAL **3**
EXECUTIVE SUMMARY **4**
GLOSSARY **5**
TABLE OF CONTENTS **6**
LIST OF TABLES **7**
LIST OF FIGURES **8**
1. Introduction **10**
2. Technical background **11**
2.1. State-of-the-art hyperspectral imaging 11
2.2. Beyond state-of-the-art: active hyperspectral imaging 11
3. Data collection **13**
3.1. Passive hyperspectral measurements in laboratory 13
3.1.1. Reference samples *13*
3.1.2. Pilot site samples *14*
3.2. Active hyperspectral measurements in laboratory 15
3.2.1. Reference samples *15*
3.2.2. Pilot site samples *16*
3.3. Active hyperspectral measurements in the pilot sites 16
3.3.1. The Hague, The Netherlands *16*
3.3.2. Longyearbyen, Svalbard *17*
4. Exploratory analysis **19**
4.1. Data pre-processing 19
4.2. Cluster analysis 20
4.3. Moisture analysis 21
4.4. Mould detection 23
5. Conclusions and outlook **24**
ACKNOWLEDGEMENTS **25**
BIBLIOGRAPHY **26**

LIST OF TABLES

Table 1: Summary of scan locations, positions and number of scans for the pilot site in The Hague. 17

Table 2: Summary of scan locations, positions and number of scans for the pilot site in Svalbard..... 18

LIST OF FIGURES

Figure 1: Setup of the Specim hyperspectral camera. HSC: hyperspectral camera; HL: halogen lamp; S: sample; W: white reflectance reference; CB: conveyor belt. 11

Figure 2: Setup of the VTT active hyperspectral sensor in the laboratory (a) and in field tests (b). Schematics of the optical system are provided in (b). AHS: active hyperspectral sensor; S: sample; W: white reflectance reference; CB: conveyor belt. PL: pump laser; OF: optical fiber; FPI: Fabry-Pérot interferometer; TO: transmission optics; RO: receiving optics; D: detector array.(c) Photo of the AHS in in the pilot test in Svalbard. 12

Figure 3: Wood samples with different paints. Photos (a-d) and false color images generated from the hyperspectral images acquired with the state-of-the-art camera (e-h). The painting codes are (a,e) PIKA-TEHO Q157; (b,f) PIKA-TEHO 303; (c,g) PIKA-TEHO Q305; (d,h) TEHO 515X. 13

Figure 4: Second set of reference samples .Eucalyptus (a,d); Pine (b,e); Spruce (c,f). Photos (a-c) and false colour images (d-f)..... 14

Figure 5: Locations of the wooden samples collected from the Svalbard pilot test. 15

Figure 6:Samples from Svalbard. (a) Photos; (b) false colour images acquired with the state-of-the-art camera. 15

Figure 7: Wood samples with different paints. Photos (a-d) and false colour images generated from the hyperspectral images acquired with the AHS (e-h). The painting codes are (a,e) PIKA-TEHO Q157; (b,f) PIKA-TEHO 303; (c,g) PIKA-TEHO Q305; (d,h) TEHO 515X. 16

Figure 8: Samples from Svalbard. (a) Photos; (b) false colour images acquired with the AHS. 16

Figure 9: Wooden beams in the target building in the pilot site in The Hague. In each panel, the left side shows a photo of the beam, and the right side (1, 2, 4) or lower side (3, 5) shows an intensity map. 17

Figure 10: Wooden beams in the target building in the pilot site in Svalbard. In each panel, the left side shows a photo of the beam, and the right side shows an intensity map. 18

Figure 11: PCA score images of sample 3 from the Svalbard set used to remove the background and irrelevant pixels. 19

Figure 12: Example of spectra before (a) and after (b) scattering correction. 20

Figure 13: UMAP cluster analysis for the hyperspectral images of the Svalbard samples. (a) Specim data; (b) AHS data. Each datapoint in the plots represents a collection of pixels with same embedding values, and the colour map indicates the density of pixels (red à more pixels with the value corresponding to the coordinates; blue à less pixels). The red circle highlights sample 4. 21

Figure 14: Principal component analysis (PCA) for the Svalbard samples before and after exposure to 95% humidity in moisture chamber. 21

Figure 15: AHS average spectra of the Svalbard samples before and after 24 h period in the 95% humidity chamber. 22

Figure 16: Specim average spectra of the Svalbard samples before and after 24 h period in the 95% humidity chamber. 22

Figure 17: PCA results of the data acquired with the AHS using average spectra. Score plot (a) and loadings (b) of the first 2 PCs. 23

Figure 18: Samples for which mould formation was observed. Photos (a,d), relative concentration colour maps generated by MCR-ALS (b,e) and pure spectra identified by the MCR-ALS (c,f)..... 23

1. Introduction

This deliverable is linked to task 2.2 of WP2 in the SUM4Re project. This task consists of generating a database of hyperspectral images relevant to assessing the quality of timber in built environments using active hyperspectral sensing (AHS). The AHS is one of the several technologies deployed to build environments in the SUM4Re project to assess different aspects of elements and materials in terms of recyclability/reuse feasibility in the context of circularity. Specifically, task 2.2 concerns Use Case (UC) 2: Characterisation of ageing timber construction components for reuse.

In the context of AHS, ageing is assessed in terms of wood deterioration, which can be characterized by detecting the presence of different types of mould/rot, or other features which can lead to deterioration, such as moisture. As a spectroscopic technique, the signals obtained with AHS reveal information about the macroscopic molecular composition of the materials. In practice, this means that the AHS should be able to identify characteristics of the material that arise from compositional changes on the order of several percent, and regarding molecular structures, not chemical elements (elemental composition can be retrieved from X-ray fluorescence, which is the topic of deliverable 2.3). AHS is a type of vibrational spectroscopy in the near infrared (NIR) spectral region, which means that the features observed in the spectra are specific to chemical bonds between atoms, and they are affected by the overall molecular structure [1]. In practice, this means that the AHS spectral signals serve as fingerprints of a given material. Therefore, the objective of this task can be understood as obtaining a database of material fingerprints, which in task 3.2 of WP3 will be used to generate qualitative or quantitative models to determine target properties of wood.

The main components of wood are cellulose, lignin and hemicellulose [2]. All these three compounds present characteristic spectral features in the near infrared (NIR) spectral region which arise from OH (oxygen-hydrogen) and CH (carbon-hydrogen) vibrational modes in the molecules. Therefore, NIR spectra of any wood consists of a combination of spectral features from these main three substances. Degradation of wood by brown or white rot changes the relative proportion of these compounds in a given sample, and this is reflected in the spectra [3]. Therefore, the premise of detecting deterioration of wood depends on measurable changes in the proportion of these three substances, which has been demonstrated with laboratory NIR and hyperspectral systems [4]. Here, we evaluate the feasibility of detecting such markers of deterioration using the VTT AHS, which can be used in field tests.

2. Technical background

2.1. State-of-the-art hyperspectral imaging

The state-of-the-art hyperspectral camera used for reference laboratory measurements was the push-broom Specim SWIR [5]. This device covers the spectral range from 1000 to 2500 nm, with a total of 288 spectral elements. The images are formed by lines containing 384 pixels, typically with a field of view of 12 cm, which leads to a pixel width of 312 µm. The images are acquired by moving a conveyor belt in the direction perpendicular to the line being scanned, at a speed of 9 mm/s and a frame rate of 25 Hz, leading to a pixel length of 360 µm. Thus, the pixel size it 312×360 µm.

The spectral resolution is 12 nm. The light source for this camera consists of a set of halogen lamps. Figure 1 shows the schematics of the Specim hyperspectral camera. The halogen lamps (HL) illuminate the objects on the conveyor belt (CB) that moves below the camera (HSC). The HSC is placed at a height that leads to a field of view of 12 cm. The white reflectance reference (W) is imaged before every sample to enable calculation of the reflectance spectrum according to Eq. 1:

$$R = \frac{I_S}{I_W - I_D} \quad (Eq. 1)$$

in which R is the reflectance, and I_S, I_W and I_D are the recorded intensities for the sample, white reflectance reference and dark, respectively. The dark signal is recorded by closing a shutter in front of the camera. The reflectance spectrum consists of a continuous function with dips, the absorption peaks. Such absorption peaks are specific to each material, and act as a "fingerprint" that allows identifying materials and their properties.

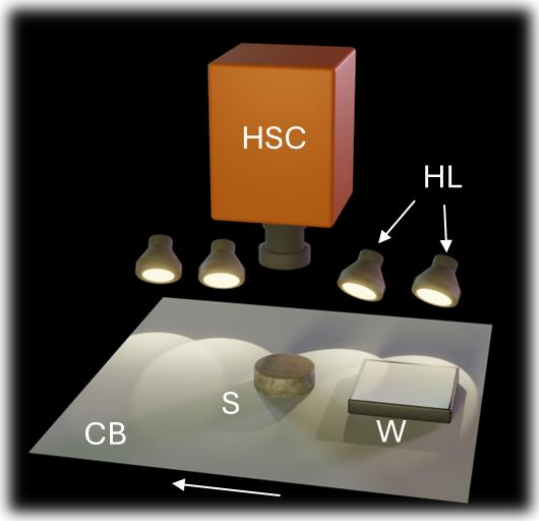

Figure 1: Setup of the Specim hyperspectral camera. HSC: hyperspectral camera; HL: halogen lamp; S: sample; W: white reflectance reference; CB: conveyor belt.

2.2. Beyond state-of-the-art: active hyperspectral imaging

Figure 2 shows the setup of the active hyperspectral sensor as used in laboratory measurements (a), in the field (b), and a photo of the real system (c). In the laboratory, the AHS was used to scan samples on a conveyor belt, similar to the state-of-the-art camera setup. The key difference, which also enables its use in the field, is the active illumination based on supercontinuum light sources. This active illumination allows for long distance measurements and robustness with respect to ambient light [6].

The schematics of the AHS is explicit in Figure 2(b). A pump laser (PL) is guided through a nonlinear supercontinuum fiber (SCF), which broadens the laser spectrum (centered at

1550 nm) leading to a spectral coverage of hundreds of nm. A microelectromechanical Fabry-Pérot interferometer (MEMS-FPI) selects and scans the wavelengths according to a voltage sweep. The light transmitted through the FPI is guided *via* the transmission optics (TO) to the target as a line beam. The reflected light is collected by the receiving optics and imaged in a line detector array. The full 2D image is acquired by scanning the line on the sample with either an external mirror accessory of with a pan-tilt mount that supports the entire AHS and moves it perpendicular to the line. Either way, the idea is analogous to the conveyor belt setup, with the difference that the AHS moves instead of the target.

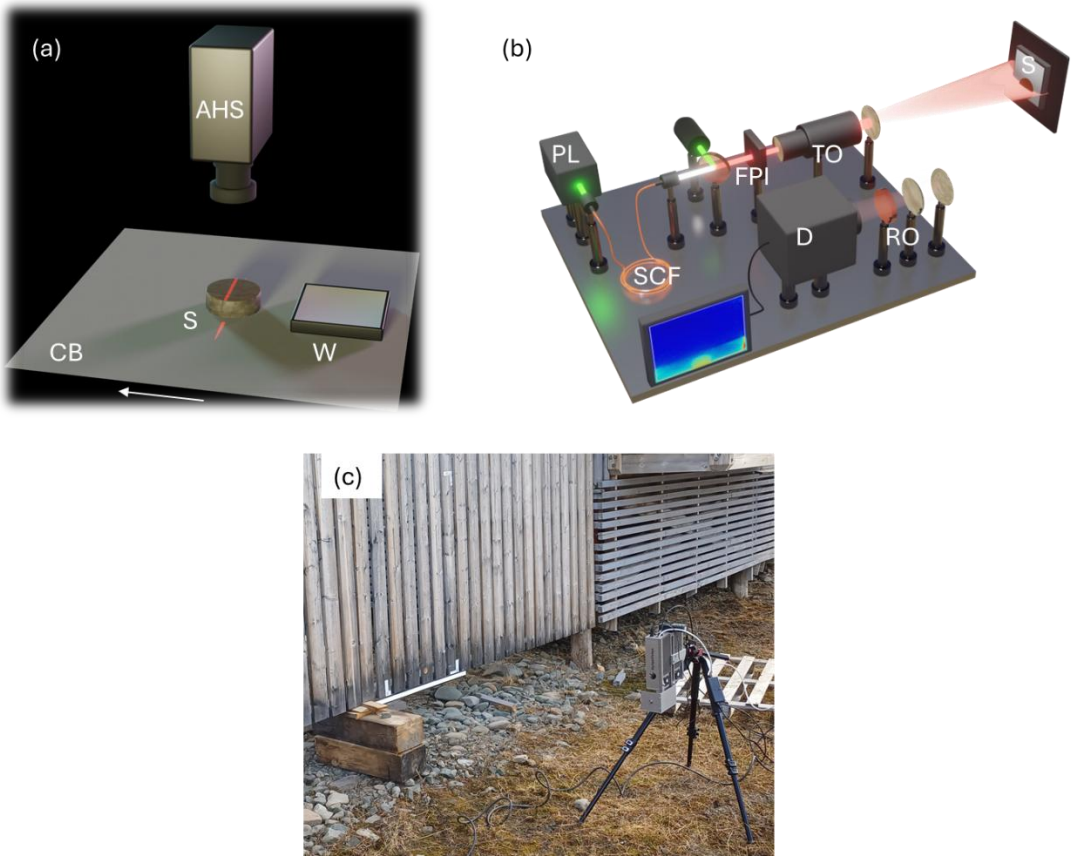

Figure 2: Setup of the VTT active hyperspectral sensor in the laboratory (a) and in field tests (b). Schematics of the optical system are provided in (b). AHS: active hyperspectral sensor; S: sample; W: white reflectance reference; CB: conveyor belt. PL: pump laser; OF: optical fiber; FPI: Fabry-Pérot interferometer; TO: transmission optics; RO: receiving optics; D: detector array.(c) Photo of the AHS in in the pilot test in Svalbard.

3. Data collection

The data collection was carried both in laboratory and onsite in the pilot tests. In laboratory, the data was collected both with the passive state-of-the-art HSI (Specim) and the AHS, and onsite only with AHS. The database consisted of measurements taken both with samples collected directly from the pilot site (in the case of Svalbard) and reference wood samples from Finland. One important remark is that although the samples from the Svalbard pilot were collected from the building, the AHS consists of a non-destructive technique (NDT). In a case where the AHS is fully calibrated, the tests can be done directly on site without any collection of samples for the site. It was only a matter of convenience in the case of the Svalbard pilot that, as it is a peculiar site, and the buildings would be demolished, we decided to collect samples directly from the location.

One of the goals of task 2.2 in SUM4Re is to build an extensive database of hyperspectral images with both AHS and the state-of-the-art device, as described in the grant agreement (GA). The data presented below was found sufficient to develop qualitative models for assessing the target properties of wood at this stage of the project. Such exploratory models are described in section 4, and include linear models such as principal component analysis (PCA) and multivariate curve resolution alternating least squares (MCR-ALS).

In the following sections, these sample sets and measurements are described.

3.1. Passive hyperspectral measurements in laboratory

3.1.1. Reference samples

The reference samples consisted of two sets. The first one included three samples of soft wood (pine/spruce) with different types of coatings and paints. Figure 3 shows photos of the samples along with the false colour images. False colour images are generated by taking selected wavelengths or average of wavelengths in the infrared range of the camera and assigning their values of reflectance to RGB coordinates. This is a way to visualize quickly the hyperspectral image in a way analogous to photos.

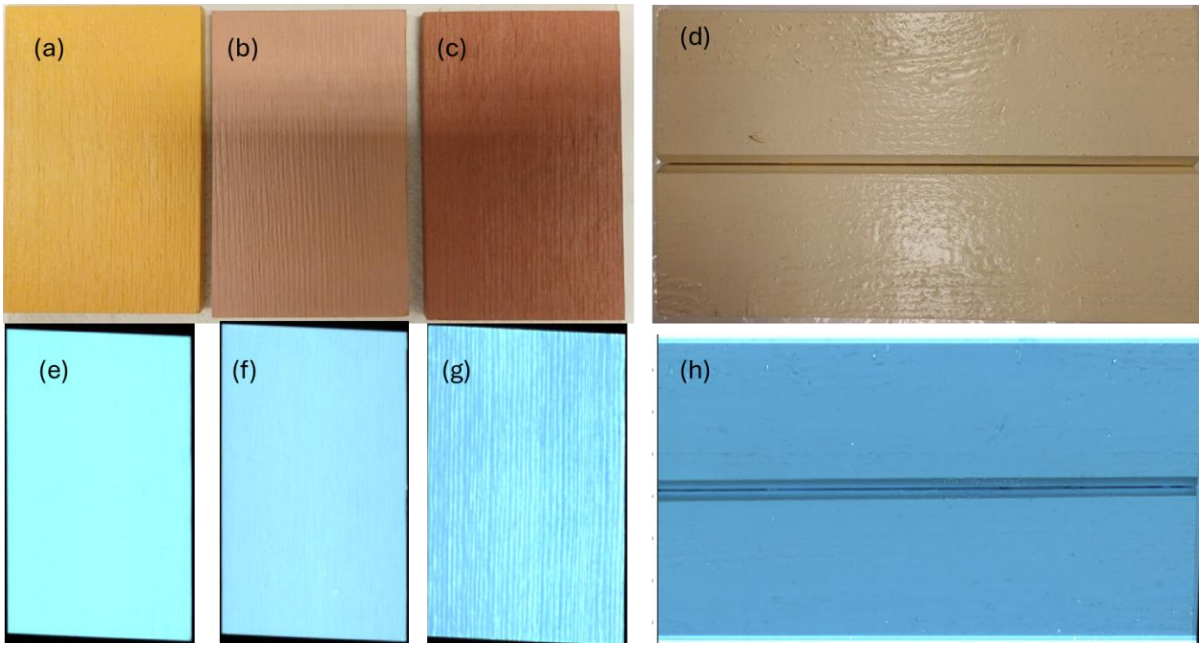

Figure 3: Wood samples with different paints. Photos (a-d) and false color images generated from the hyperspectral images acquired with the state-of-the-art camera (e-h). The painting codes are (a,e) PIKA-TEHO Q157; (b,f) PIKA-TEHO 303; (c,g) PIKA-TEHO Q305; (d,h) TEHO 515X.

The second set consisted of samples of different types of wood without any painting or treatment. Figure 4 shows the photos of the samples along with the false colour images.

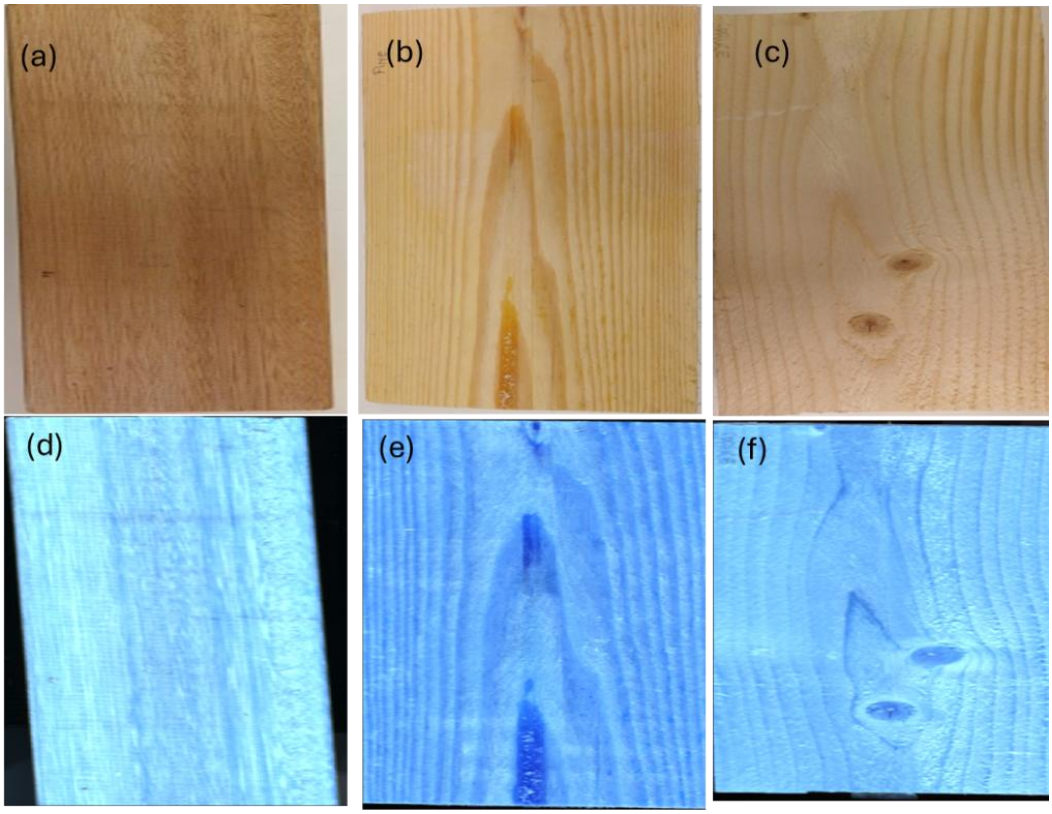

Figure 4: Second set of reference samples .Eucalyptus (a,d); Pine (b,e); Spruce (c,f). Photos (a-c) and false colour images (d-f).

3.1.2. Pilot site samples

A set of 10 samples was obtained directly from the Svalbard pilot. Both sides of the samples were imaged to account for differences related to coatings/paintings, as the hyperspectral sensors scan only the surface. In total, this procedure lead to 20 individual hyperspectral images. Wooden disks of 25 mm diameter were collected from different parts of the test building. The locations from where the disks were extracted are illustrated in Figure 5, and the samples themselves are shown in Figure 6. False colour images for these samples were generated in way described in the previous paragraph. It is noteworthy that the Svalbard samples visibly present more variability due to the absence of paint in some of the samples, unlike the reference ones in Figure 3.

Figure 5: Locations of the wooden samples collected from the Svalbard pilot test.

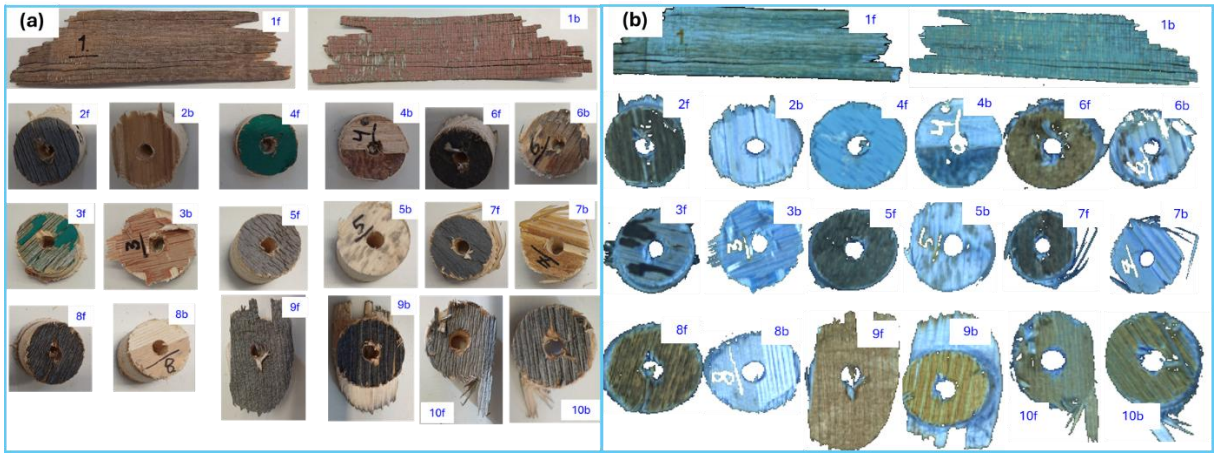

Figure 6:Samples from Svalbard. (a) Photos; (b) false colour images acquired with the state-of-the-art camera.

Since the buildings in The Hague are in use (both target and donor buildings), no samples were collected directly from that location. More info regarding this pilot site can be found in deliverable 10.2.

3.2. Active hyperspectral measurements in laboratory

3.2.1. Reference samples

For the AHS measurements, only the first set of samples was measured so far. The second set of untreated samples will be included in the deliverable 3.2, along with the full data analysis results. Figure 7 shows the photos of the first set of reference samples compared to the false colour images acquired with the AHS. The hyperspectral images present a striped pattern, which is an artifact of the measurement. This problem was corrected and did not appear in the following measurements.

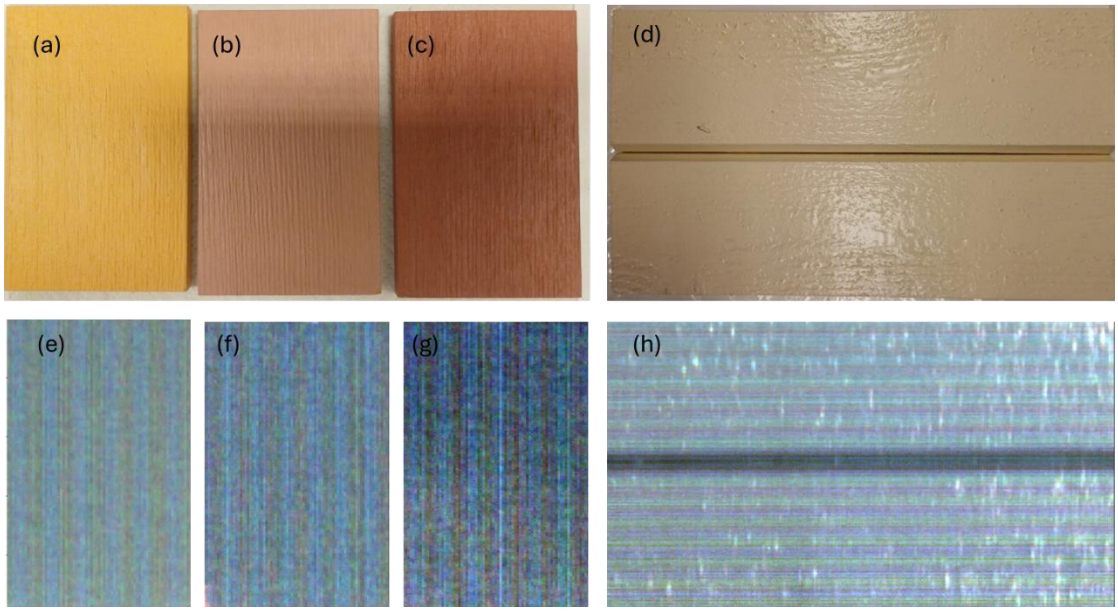

Figure 7: Wood samples with different paints. Photos (a-d) and false colour images generated from the hyperspectral images acquired with the AHS (e-h). The painting codes are (a,e) PIKA-TEHO Q157; (b,f) PIKA-TEHO 303; (c,g) PIKA-TEHO Q305; (d,h) TEHO 515X.

3.2.2. Pilot site samples

Figure 8 shows the photos and false colour images acquired with the AHS for the samples obtained from the Norwegian pilot site in Svalbard. Compared to the images acquired with the state-of-the-art camera, the false colour images appear more almost monochromatic. This is due to the narrower spectral range of the AHS, which is dominated by one absorption features at around 1420 nm.

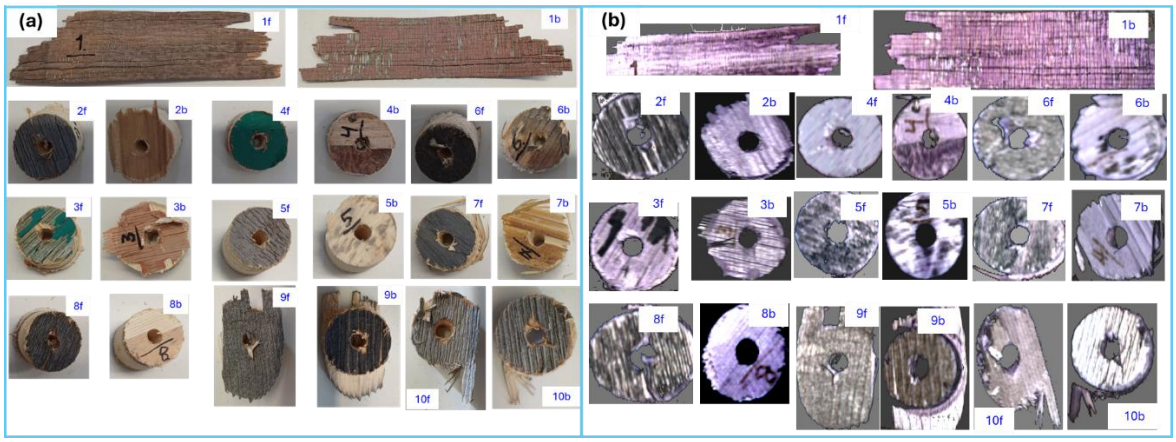

Figure 8: Samples from Svalbard. (a) Photos; (b) false colour images acquired with the AHS.

3.3. Active hyperspectral measurements in the pilot sites

In this section we present some images of the measurements carried out in the pilot tests in the Binckhorst district in The Hague, Netherlands and in Longyearbyen, in the island of Svalbard, Norway. In this deliverable we focus on the hyperspectral images. Details regarding measurement procedures, planning and description of the pilots are provided in deliverables 10.2 and 10.3.

3.3.1. The Hague, The Netherlands

The location selected for scanning with the AHS in the pilot site in The Hague was the attic of the target building. The first reason for this selection was that this is the only place where

wooden beams were available to be scanned. The second reason was that this location is safer, since there are no people circulating the area. More details of the building and description of the pilot test are given in deliverable 10.2.

Figure 9 shows the hyperspectral images and photos of the scanned wooden beams. The hyperspectral images here are depicted as intensity maps of one average wavelength, unlike the false colour images. This is the type of data visualization implemented in the AHS software during the data acquisition and serves the purpose of checking the overall intensity of the signal and signal-to-noise-ratio (SNR). As seen in Figure 9, multiple scans of each location were acquired. This was done maximize the areas of scan, as there is a limit of the scanning angle of the mirror in the AHS, and the device needs to be moved to extend the area. Replica scans were also acquired to test how the SNR can be improved by averaging, and to minimize risks of faulty pixels or lines. For clarity, only two scans for each target are shown in Figure 9. The full list of scans is provided in Table 1.

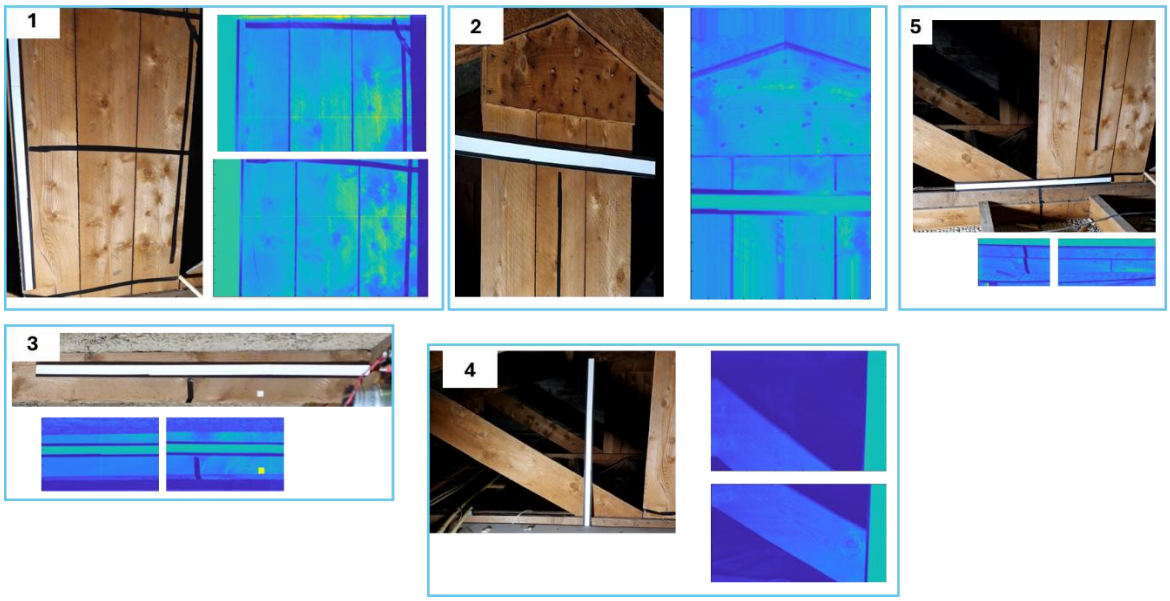

Figure 9: Wooden beams in the target building in the pilot site in The Hague. In each panel, the left side shows a photo of the beam, and the right side (1, 2, 4) or lower side (3, 5) shows an intensity map.

Table 1: Summary of scan locations, positions and number of scans for the pilot site in The Hague.

Target beam	Number of positions	Total number of scans
1	4	7
2	3	7
3	3	6
4	3	6
5	2	4

3.3.2. Longyearbyen, Svalbard

The location of the scanning areas in the Svalbard pilot were defined in deliverable 10.3 in agreement with all the partners involved in the pilot. Here we report only the hyperspectral images and their corresponding locations. For a comprehensive view and description of the locations, including blueprints, see deliverable 10.3.

Figure 10 shows the photos of the scanning areas in the Svalbard pilot. Similarly to Figure 9, the photos are presented next to the intensity maps, and not false colour images. In the case of Svalbard pilot, the number of scans is larger because there were some issues with communication between the AHS and the controlling laptop during the field test. For this reason, some scans contained many missing or faulty lines and had to be repeated. In addition, replica scans were carried out to test the extent of which the SNR can be improved by averaging.

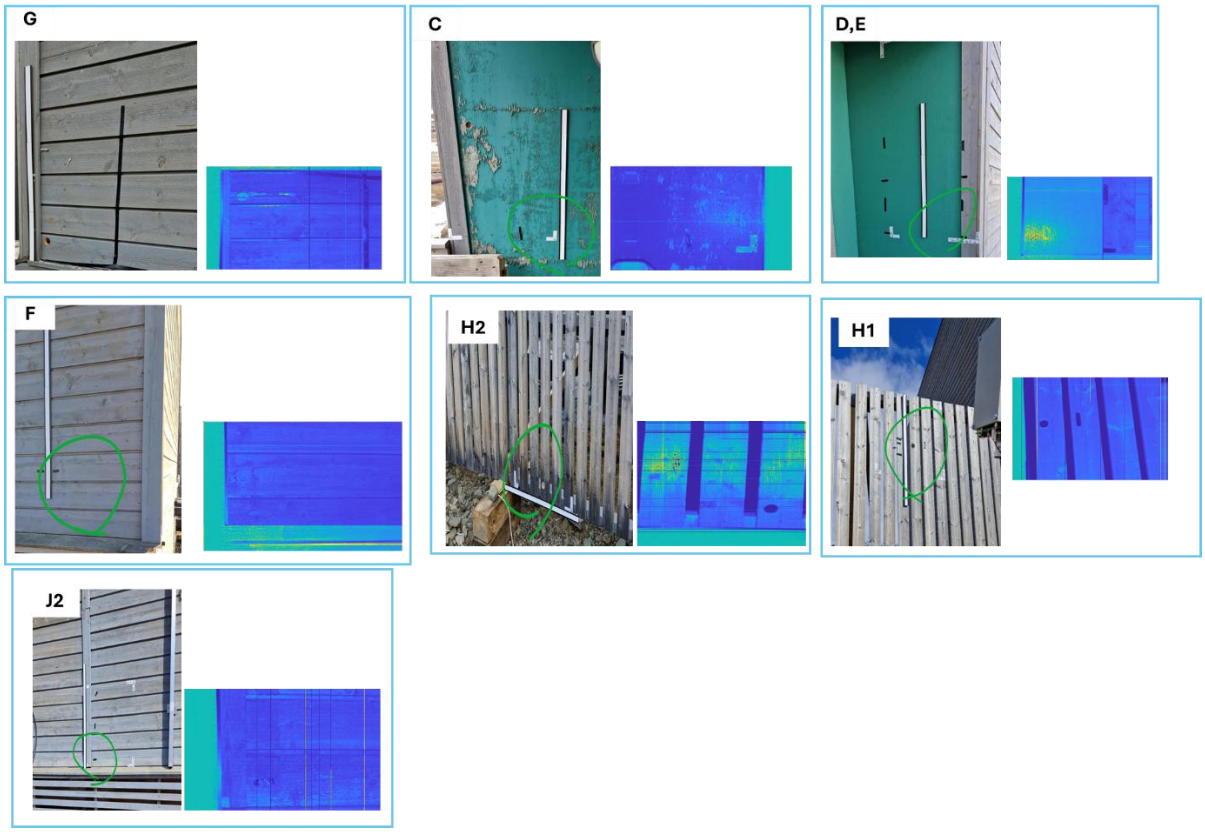

Figure 10: Wooden beams in the target building in the pilot site in Svalbard. In each panel, the left side shows a photo of the beam, and the right side shows an intensity map.

Table 2: Summary of scan locations, positions and number of scans for the pilot site in Svalbard.

Target location (according to code reported in deliverable 10.3)	Number of positions	Total number of scans
G	3	15
C	6	24
D,E	4	8
F	4	8
H2	2	9
H1	1	2
J2	2	6

4. Exploratory analysis

This section describes the exploratory data analysis methods used in task 2.2. Here we emphasize that the linear methods (PLS.PLS-DA) mentioned in the GA were merely examples of methods typically used for hyperspectral imaging but were actually not needed for the application. Instead, we used other methods such as principal component analysis (PCA), multivariate curve resolution alternating least squares (MCR-ALS), as described in the following subsections. Additionally, the AI methods mentioned in the GA (ANN, SVM) were not employed here, as they would not be applicable to the number of measurements, and would not be required. In the continuation task T3.2, we will further evaluate the need to implement such AI models, as in that task we will refine the data analysis with the purpose of providing the final valuable information for C-BIM.

4.1. Data pre-processing

Prior to data analysis, the hyperspectral images must be processed to remove faulty pixels/irrelevant parts of the image (e.g. background) and mitigate optical artifacts (e.g. scattering). This processing consists of both image and spectral processing steps. The specific procedure for the hyperspectral images of the samples and target elements in the pilot building sites is described below:

1. Image background and irrelevant pixel removal. Using the raw reflectance image, we perform principal component analysis in all pixels to generate a score image, analogous to the false colour image. In this score image, we can visualize outlier pixels as well as the background and set a threshold for score values to remove undesired parts of the image. This procedure is illustrated in Figure 11 for sample 3 of the Svalbard samples. The scores of both background and the ink marking the sample number are distinct from the wood and appear as purple in the score image (a), so they can be easily removed by setting an appropriate threshold for the PCA scores (b).

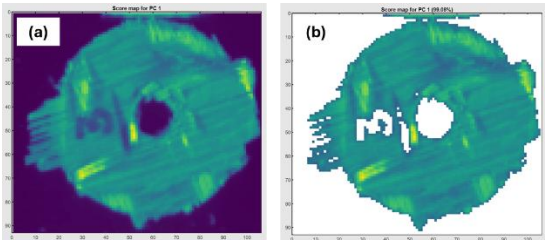

Figure 11: PCA score images of sample 3 from the Svalbard set used to remove the background and irrelevant pixels.

2. Conversion to absorbance. The Lambert-Beer law states that the concentration of a given analyte is directly proportional to the inverse logarithm of transmittance in transmission spectroscopy. In reflectance spectroscopy, the absorbance can be approximated by the inverse logarithm of reflectance, according to Eq. 2. We applied this conversion to all spectra to improve the quality of linear models to be applied as further steps.

$$A = \log R \quad (Eq. 2)$$

3. Baseline removal/scattering correction/denoising. The spectra of each pixel are affected by optical effects which are not related to material chemical properties, but rather to surface roughness and the angle of incidence of light. In addition, noise from various sources can hinder the clarity of the useful spectral features. In the data presented in this report, the preprocessing consisted of the following steps:
   a. Denoising: Second degree Savitzky-Golay smoothing;
   b. Baseline removal/scattering correction: First derivative.

   Figure 12 shows spectra of few pixels of sample 3 of the Svalbard set before and after preprocessing.

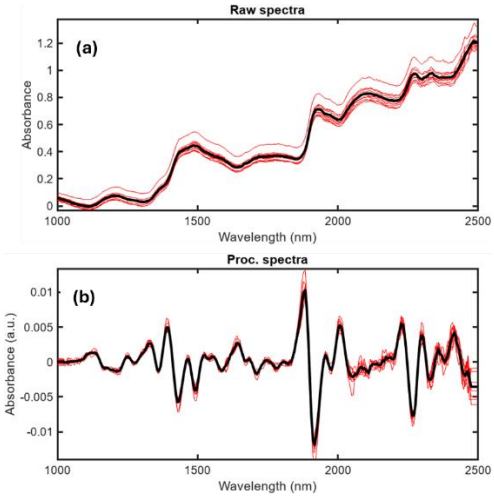

Figure 12: Example of spectra before (a) and after (b) scattering correction.

For the hyperspectral images analysed for the presence of mould with multivariate curve resolution alternating least squares method (MCR-ALS), the baseline removal method was asymmetric least squares. This was done because the MCR-ALS requires only non-negative values in the spectra, and this method of baseline removal sets he baseline at zero.

4. Averaging. In some cases, it was necessary to take the average spectrum across all pixels of one sample to improve the signal-to-noise ratio (SNR) and enable better interpretation of results.

4.2. Cluster analysis

We deployed two methods of dimensionality reduction to identify sources of variability and patterns/clusters in the hyperspectral data: PCA and uniform manifold approximation and projection (UMAP). Both methods are unsupervised, i.e. they do not generate the clusters based on any assumptions provided as input parameter or reference information. Therefore, they are useful to understand what the data can potentially provide given its variability, before any comparisons to reference data are made. Typically, if no patterns of clusters are observed in this exploratory step, it is likely that the data is either too noisy or it does not contain useful information.

The first method was PCA, but this time, applied to the pre-processed data, and not the raw data as described in section 0. Although PCA was able to identify patterns, the best method to separate the pixels of the samples in clusters was UMAP. Figure 13 shows the UMAP embeddings plots for the hyperspectral images acquired with the Specim camera (a) and the AHS (b). The large difference in the cluster structure is likely due to the wider spectral range of the Specim camera, which allows for identification of more features that differentiate the samples. Nevertheless, the AHS data reveals four separate clusters. In both cases, sample four stands out as an isolated cluster. The reasons why sample four appears to be an outlier will be investigated further in WP3, but some preliminary discussion is provided in section 4.4.

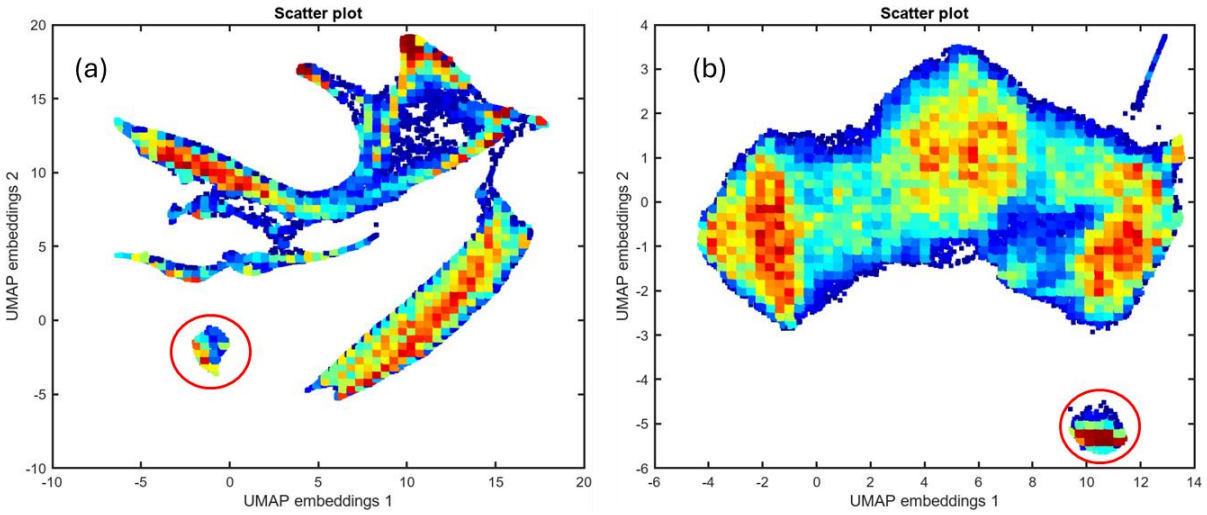

Figure 13: UMAP cluster analysis for the hyperspectral images of the Svalbard samples. (a) Specim data; (b) AHS data. Each datapoint in the plots represents a collection of pixels with same embedding values, and the colour map indicates the density of pixels (red à more pixels with the value corresponding to the coordinates; blue à less pixels). The red circle highlights sample 4.

4.3. Moisture analysis

To verify the effect of moisture in the hyperspectral images, we exposed the Svalbard set of samples to 95% relative humidity in a moisture chamber. The samples were left inside the chamber for at least 24 h, to ensure complete absorption of water. The saturation was verified by checking the increase of mass of the samples.

Figure 14 shows a score plot of PCA analysis carried out for the hyperspectral images before (dry) and after exposure to 95% humidity (wet). Overall, no clear differences are observed in the scores. This is intriguing, as water presents a strong absorption feature around 1420 nm, which should enable distinction of these groups. Some factors may explain this finding, including the heterogeneity of the wood surface (the analysis was carried out for individual pixels), low signal-to-noise ratio (SNR) at the single spectrum level, and overlapping features related to OH vibrational modes in wood. As some of the main components of wood (e.g. cellulose) contain OH groups, multiple compositional changes may contribute to the variance related to the band around 1420 nm.

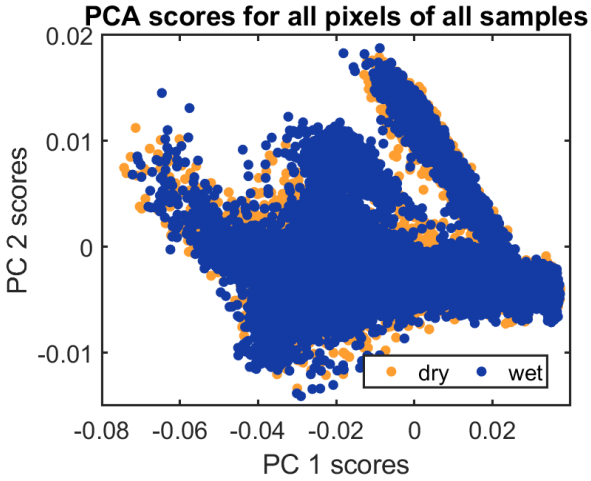

Figure 14: Principal component analysis (PCA) for the Svalbard samples before and after exposure to 95% humidity in moisture chamber.

In Figure 15 and Figure 16, the average spectra of the samples before (dry) and after being exposed to 95% humidity (wet) are compared for each sample. From the plots, the reason why the PCA is unable to separate the samples in two groups is clear: the increase of the

water peak does not happen for all samples after exposure to humidity. This effect is observed for both the data using the Specim camera and the AHS. Considering the level of noise is higher at individual pixel level, it is understandable that the PCA done for all pixels is unable to identify any patterns.

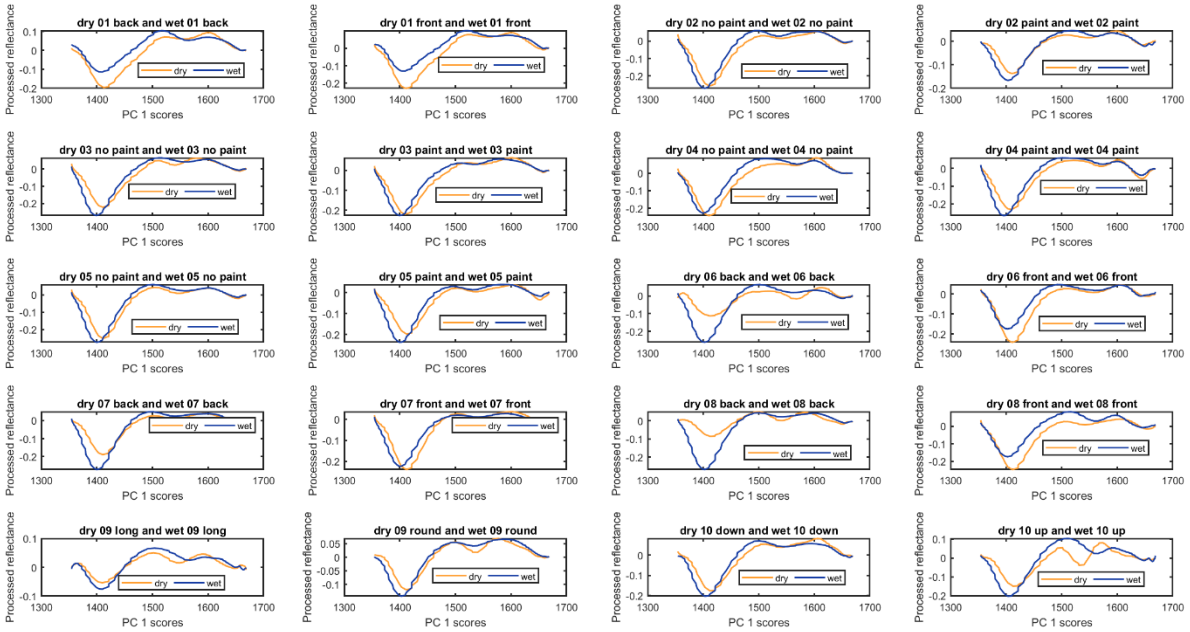

Figure 15: AHS average spectra of the Svalbard samples before and after 24 h period in the 95% humidity chamber.

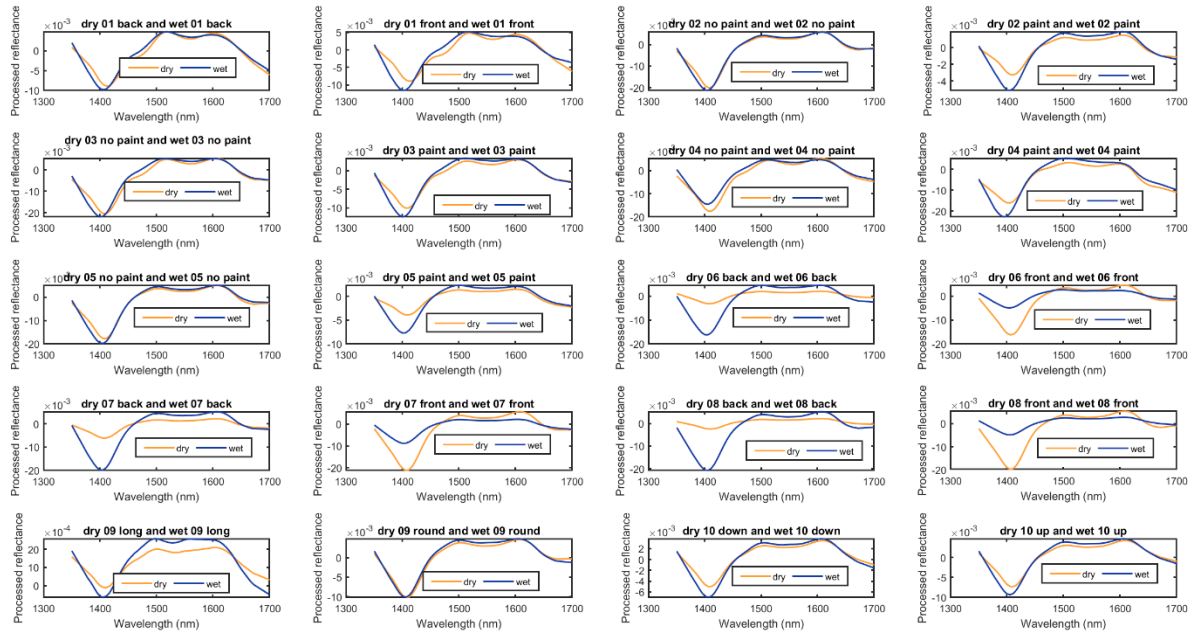

Figure 16: Specim average spectra of the Svalbard samples before and after 24 h period in the 95% humidity chamber.

Despite the different behaviour among the samples, the PCA performed on the average spectra shows a clear separation between the wet and dry samples, as shown in Figure 17. The samples appear in two separate groups, even though the separation is not so drastic. Moreover, the PC that separates best the samples is PC 2. The loadings of PC 2, which indicate the wavelengths most represented in that PC, have a broad valley around the region

of the water absorption peak. This is consistent with the score plot, in which the dry samples present more positive values and the wet samples more negative values.

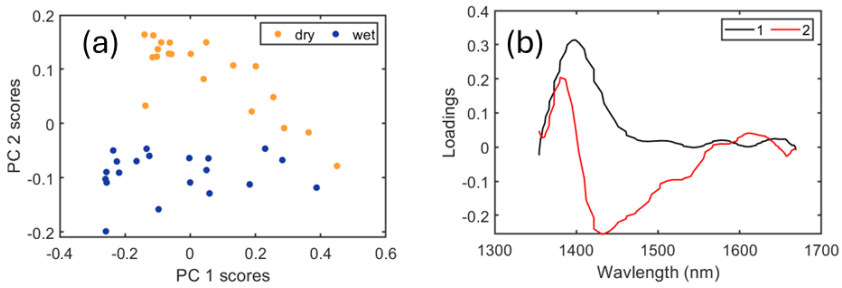

Figure 17: PCA results of the data acquired with the AHS using average spectra. Score plot (a) and loadings (b) of the first 2 PCs.

4.4. Mould detection

Figure 18 shows some of the samples after exposure to 95% moisture. In samples 3 and 4 two types or rot appeared in the samples, likely due to mould. The hyperspectral images were analysed using the multivariate curve resolution alternating least squares (MCR-ALS) method, which enables mapping the relative concentration of assumed pure components in the image without any reference information. MCR-ALS is ideal in cases where it is not possible to have reference information for individual pixels, or not at all.

The results in Figure 18 show that the MCR-ALS was able to identify one pure spectral component linked to the regions where the mould is visible in the sample and map the concentration of this component in the entire image. For both samples, the spectral features of the pure component reflect the overall shape of the spectrum of wood. This is expected, considering that the mould itself should not be identifiable by spectroscopy in the NIR region. Rather, what should be characteristic of spectra in the regions where the mould has deteriorated the wood are changes due to the alterations in the relative quantities of the wood components, i.e. cellulose, hemicellulose and lignin. Reference analysis should be carried in the future, to confirm that this is case with these samples.

It is also noticeable that the concentration maps do not match exactly the location of mould in the photo. This could indicate that hyperspectral imaging is useful to detect mould even where it is not visible, but it could as well be due to the overlapping features of wood. Again, reference analysis would be required to confirm either one of these hypotheses.

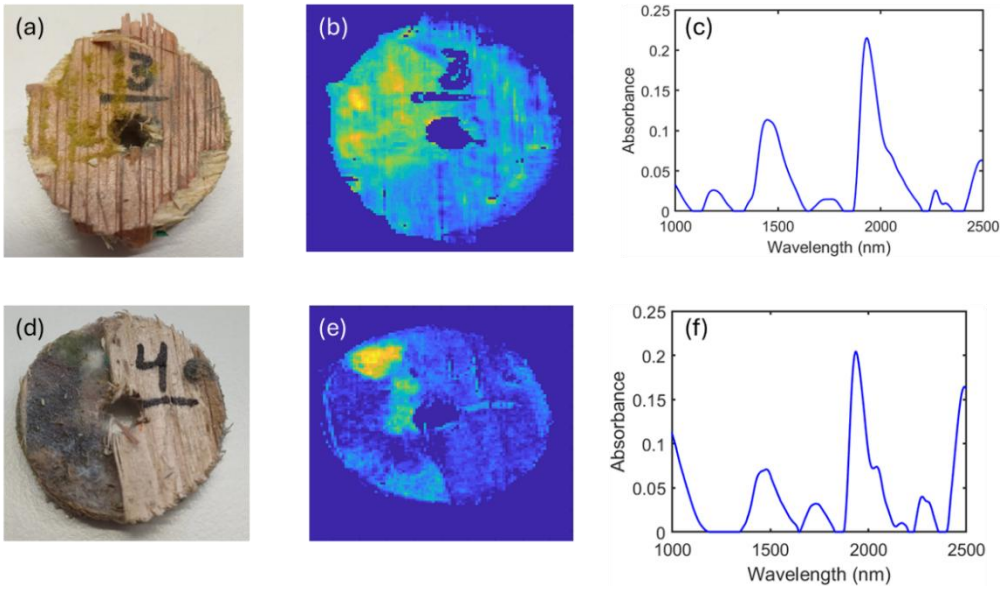

Figure 18: Samples for which mould formation was observed. Photos (a,d), relative concentration colour maps generated by MCR-ALS (b,e) and pure spectra identified by the MCR-ALS (c,f).

5. Conclusions and outlook

In this deliverable, we presented an overview of the collected data for building a database for future analysis in task 3.2 in WP3. The only missing data set for AHS is the second set of reference samples, which will be measured shortly and included in the following deliverable 3.2 with the full data analysis. Our preliminary analysis indicates the potential of AHS to assess the deterioration of wood in built environments, as well as moisture and identification of different wood types and conditions.

The main concern raised here is the challenges to detect mould with AHS, as the MCR-ALS required the full SWIR spectral range to map the mould in both samples in which it was detected. However, this problem might be tackled in the next steps by including reference analysis and testing quantitative methods.

The hyperspectral data from the pilot test sites is presented in this deliverable without an in depth quantitative and qualitative analysis. A complete data analysis of the hyperspectral images of these measurements will be presented in deliverable 3.2, in which a more thorough analysis of the samples will also be provided.

ACKNOWLEDGEMENTS

The SUM4Re research project is funded by the European Union under Horizon Europe Grant Agreement number 101129961. Views and opinions expressed are however those of the author(s) only and do not necessarily reflect those of the European Union. Neither the European Union nor the granting authority can be held responsible for them. Under number agreement

BIBLIOGRAPHY

[1] Pasquini, C. *Near Infrared Spectroscopy: Fundamentals, Practical Aspects and Analytical Applications* (2003). In: Journal of Brazilian Chemical Society (14), 2 198-219.

[2] Salmén, L, Burgert, I. *Cell wall features with regard to mechanical performance. A review.* (2009). In: Holzforschung (63), 121-129.

[3] Fackler, K., Schwanninger, M. *How spectroscopy and microspectroscopy of degraded wood contribute to understand fungal wood decay.* (2012). In: Applied Microbiology and Biotechnology (96), 587-599.

[4] Jochemsen, A., Alfredsen, G., Burud, I. *Hyperspectral imaging as a tool for profiling basidiomycete decay of Pinus sylvestris L.* (2022). In: International Biodeterioration & Biodegradation. 105464.

[5] https://www.specim.com/products/swir/

[6] Kääriäinen, T., Jaanson, P., Vaigu, A., Mannila, R., Manninen, A. *Active Hyperspectral Sensor Based on MEMS Fabry-Pérot Interferometer* (2019). In: Sensors. (19) 2192.

SUM4Re

Creating materials banks
from digital urban mining

www.sum4re.eu sum4re@uvigo.gal SUM4Re SUM4Re_EU

Funded by the European Union. Views and opinions expressed are however those of the author(s) only and do not necessarily reflect those of the European Union. Neither the European Union nor the granting authority can be held responsible for them.

Funded by the European Union